frontiers | Frontiers in Materials

ORIGINAL RESEARCH
published: 22 June 2022
doi: 10.3389/fmats.2022.937437

Radar Cross Section Approach in Illusion Effects of Transformation Optics-Based Expander

Mohammad Mehdi Sadeghi *

Department of Physics, Jahrom University, Jahrom, Iran

In this paper, analytical calculation has been provided to show illusion perception in electromagnetics expander. For this end, a precise analytical solution has been done for a scattered wave from the expander including an object in the core medium. Also, this analytical calculation has been done for a bare transformed object with different size and constitute parameters (CPs). Illusion perception, in the far field, can be illustrated by comparing the calculated scattered field patterns (SFP) of the object placed inside the expander with SFP of the bare transformed object. Moreover, the same calculation and comparison has been done for nearfield SFP. In continuation, for precise deduction, radar cross sections (RCSs) of both objects have been calculated and plotted using MATLAB. Well functionality in illusion perception has been obtained using comparisons in both analytical SFPs parts and RCSs parts.

Keywords: illusion optics, radar cross section, electromagnetics wave expander, scattering theory, transformation optics

OPEN ACCESS

Edited by:
Fei Sun,
Taiyuan University of Technology, China

Reviewed by:
Shuomin Zhong,
Ningbo University, China
Yichao Liu,
Taiyuan University of Technology, China

***Correspondence:**
Mohammad Mehdi Sadeghi
Sadeghi@jahromu.ac.ir

Specialty section:
This article was submitted to Metamaterials, a section of the journal Frontiers in Materials

Received: *06 May 2022*
Accepted: *06 June 2022*
Published: *22 June 2022*

Citation:
Sadeghi MM (2022) Radar Cross Section Approach in Illusion Effects of Transformation Optics-Based Expander. Front. Mater. 9:937437. doi: 10.3389/fmats.2022.937437

INTRODUCTION

Transformation optics theory (Leonhardt, 2006; Pendry et al., 2006) was introduced in 2006, and since then it has attracted a great deal of scientific attention in theoretical and experimental (Schurig et al., 2006; Chen and Chan, 2007; Chen et al., 2008; Kwon and Werner, 2008; Luo et al., 2008; Rahm et al., 2008; Yan et al., 2008; Chen et al., 2009; Cheng et al., 2009; Lai et al., 2009; Narimanov and Kildishev, 2009; Roberts et al., 2009; Chen et al., 2010a; Chen et al., 2010b; Jiang et al., 2010; Jiang et al., 2011; Li et al., 2011; Mei et al., 2011; Li et al., 2013; Jiang et al., 2014; Sadeghi et al., 2014; Sadeghi et al., 2015a; Sadeghi et al., 2015b; Xu and Chen, 2015; Forouzeshfard and Hosseini Farzad, 2018; Liu et al., 2019; Sadeghi, 2020; Zhao et al., 2022) aspects. This theory applies coordinate transformation and metamaterials to provide desired form variations for the CP to manipulate electromagnetic waves path and direct it in the chosen manner. Hence, this theory provides a great ability to design and construct new composite artificial devices using metamaterials with various extraordinary applications. Among all these different devices, some of them also exhibit interesting illusory optical properties (Lai et al., 2009; Jiang et al., 2010; Li et al., 2011; Forouzeshfard and Hosseini Farzad, 2018; Liu et al., 2019; Sadeghi, 2020; Zhao et al., 2022). In this paper we use analytical calculation for illusion perception in transformation-based expander. For this purpose, in next section we present a transformation function to create and design a wave expander. Next, we provide a close solution in wave expansion form for SFP of an object that has been placed in the core medium of transformation-based expander. In order to show the illusion effect of this device, we compare this SFP of the object inside the expander with the SFP of a transformed bare object. Also, to illustrate the illusion effect more precisely, we provide a comparison in RCSs of both objects. Finally, we provide the conclusion in the end.

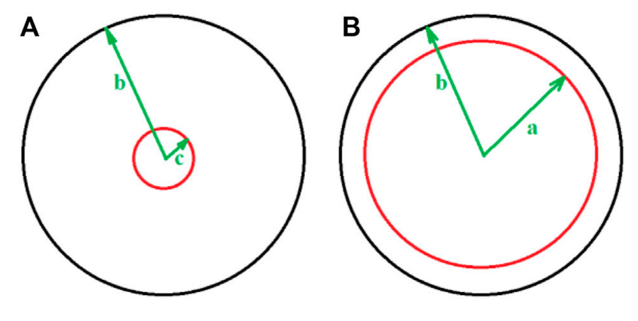

FIGURE 1 | schematic functionality of transformation function that expand **(A)** virtual region [0, c] to **(B)** real space [0, a].

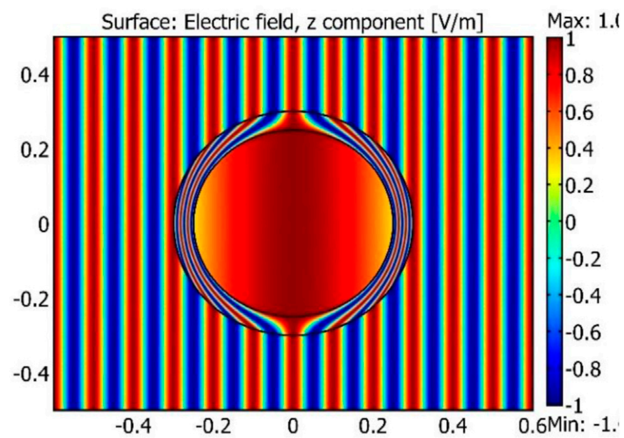

FIGURE 2 | field distribution of a TE incident wave with working frequency 1GHZ, $a = 0.25\,m$, $b = 0.3m$ and.$c = 0.02m$.

General Preliminarily

We start with a transformation function that expands the region $[0, c]$ of virtual space into region $[0, a]$ of real space as shown in **Figure 1**. This function can be provided as follow,

$$r = \begin{cases} \dfrac{a-b}{c-b} r' + b\dfrac{c-a}{c-b} & for \;\; c \le r' \le b \\ \dfrac{a}{c} r' & for \;\; 0 \le r' \le c \end{cases} \tag{1}$$

Where r and r' show the real and virtual space respectively.

According transformation optics theory we have CP of core medium i.e., $[0, a]$ of wave expander as follow,

$$\varepsilon_{core} = \mu_{core} = \begin{bmatrix} 1 & 0 & 0 \\ 0 & 1 & 0 \\ 0 & 0 & \left(\dfrac{c}{a}\right)^2 \end{bmatrix} \tag{2}$$

Likewise, for surrounding shell i.e., $[a, b]$, of wave expander we have,

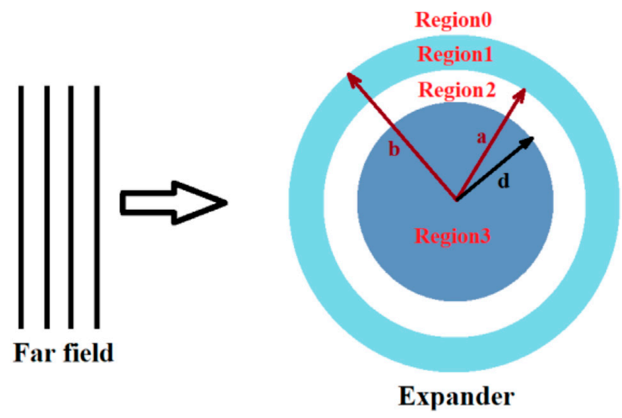

FIGURE 3 | Schematic plan for a cylindrical sample with radius d. ε_{sample} and μ_{sample} are the CP of the object that placed in core medium of expander and illuminated by planewave.

$$\varepsilon_{shell} = \mu_{shell} = \begin{bmatrix} \left(\dfrac{a-b}{c-b}\right)\dfrac{r'}{r} & 0 & 0 \\ 0 & \left(\dfrac{c-b}{a-b}\right)\dfrac{r}{r'} & 0 \\ 0 & 0 & \left(\dfrac{c-b}{a-b}\right)\dfrac{r'}{r} \end{bmatrix} \tag{3}$$

Now with these core and shell parameters and using an incidenting TE-z plane wave, the functionality of the device can be plotted as shown in **Figure 2**. The field distribution pattern of a TE incident plane wave with working frequency 1 GHZ, $a = 0.25\,m$, $b = 0.3m$ and $c = 0.02m$ has been plotted in **Figure 2** the device remains invisible and the wave expands in the core medium. However, this device can be used to create an illusion that has been presented in the next section.

RCS APPROACH

In this section we focus on illusion perception using exact solutions in the wave equation of scattering waves. For this end we put a cylindrical object with radius $d = 0.1m$ and relative CP, $\varepsilon = \varepsilon_{sample}$ and $\mu = \mu_{sample}$ in core medium in order to see the field pattern. Noteworthy we choose the sample in cylindrical shape to provide an exact analytical solution in the wave equation. In the following, we provide a solution in illusion scattering for far field and near field separately.

Consider a TE plane wave propagating in x direction as shown in **Figure 3**. Hence, we can present wave expansion outside and inside the device using boundary condition (BC). This TE plane wave can be formulated as below,

$$E = \mathcal{E} e^{ik_0 x - i\omega t} \tag{4}$$

Where k_0 and ω are the wave number and frequency of incidenting waves in the host, respectively. also $\mathcal{E}$, is the amplitude of incidenting wave. We calculate the total field in all regions using general wave equation as below:

For the electric field outside the device i.e., region0 or $\rho > b$, we have incidenting wave and scattering wave as below,

$$E_0 = \mathcal{E} \sum_{n=-\infty}^{n=\infty} [i^{-n} J_n(k_0\rho) + C_{0,n} H_n^1(k_0\rho)] e^{in\varphi} \tag{5}$$

Where J_n and H_n^1 are Bessel and Hankel function of first kind, respectively. $C_{0,n}$ is the unknown expansion coefficients of scattered part of the total field outside the device. Also, inside the device in shell region i.e., region1, we can present,

$$E_1 = \mathcal{E} \sum_{n=-\infty}^{n=\infty} [A_{1,n} J_n(k_1\rho) + C_{1,n} H_n^1(k_1\rho)] e^{in\varphi} \tag{6}$$

For the core medium i.e., region2, we have the wave as follow,

$$E_2 = \mathcal{E} \sum_{n=-\infty}^{n=\infty} [A_{2,n} J_n(k_2\rho) + C_{2,n} H_n^1(k_2\rho)] e^{in\varphi} \tag{7}$$

And finally, for inside the sample i.e., region3, that has been inserted inside the core medium we have,

$$E_3 = \mathcal{E} \sum_{n=-\infty}^{n=\infty} [A_{3,n} J_n(k_3\rho)] e^{in\varphi} \tag{8}$$

Where in **Eqs 9–11** A and C are unknown expansion coefficients. Also k_1, k_2 and k_3 are the wave vectors in corresponding regions. Now by matching of the boundary condition (BC) for continuity of electric and magnetic field at all interfaces we calculate the unknown coefficients. For three interfaces, as shown in **Figure 3**, we can provide three equations for continuity of electric field and three equations for continuity of magnetic field using $H_\varphi = \frac{1}{i\omega\mu} \frac{\partial E_z}{\partial \rho}$.

For continuity of electric fields at $\rho = b$,

$$A_{0,n} J_n(k_0 b) + C_{0,n} H_n^1(k_0 b) = A_{1,n} J_n(k_1 b) + C_{1,n} H_n^1(k_1 b) \tag{9}$$

For continuity of electric fields at $\rho = a$,

$$A_{1,n} J_n(k_1 a) + C_{1,n} H_n^1(k_1 a) = A_{2,n} J_n(k_2 a) + C_{2,n} H_n^1(k_2 a) \tag{10}$$

And for continuity of electric fields at boundary of object inside the core medium, $\rho = d$,

$$A_{2,n} J_n(k_2 d) + C_{2,n} H_n^1(k_2 d) = A_{3,n} J_n(k_3 d) \tag{11}$$

We use similar BCs for continuity of magnetic fields at all boundaries.

For continuity of magnetic fields at $\rho = b$,

$$\frac{k_0}{\mu_0}\left(A_{0,n} J'_n(k_0 b) + C_{0,n} H_n^{1'}(k_0 b)\right) = \frac{k_1}{\mu_1}\left(A_{1,n} J'_n(k_1 b) + C_{1,n} H_n^{1'}(k_1 b)\right) \tag{12}$$

For continuity of magnetic fields at $\rho = a$,

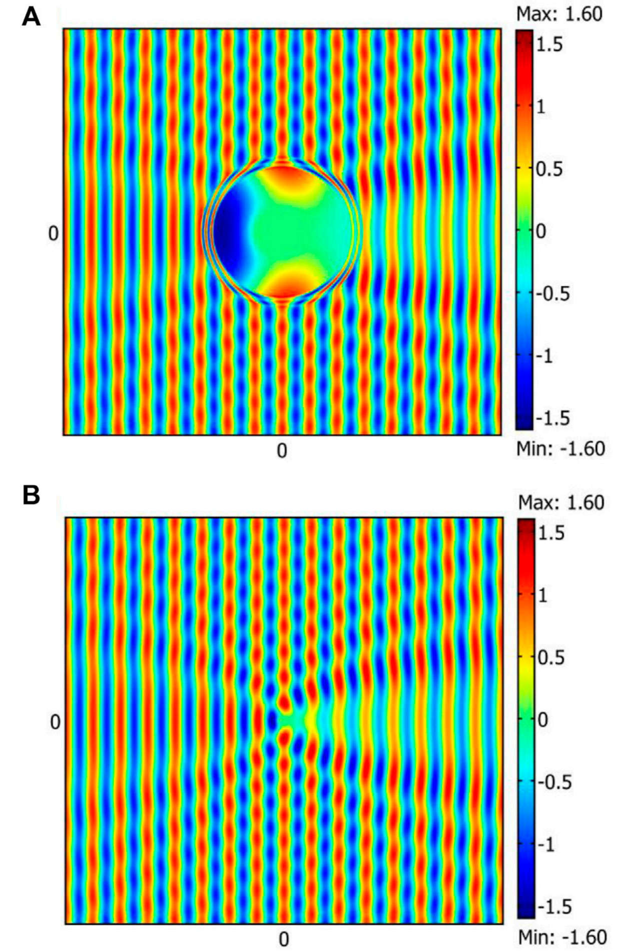

FIGURE 4 | (A) SFP of object placed in core medium of expander illuminated by far field, with $b = 0.3m$, $a = 0.25m$ and $c = 0.05m$ and $d = 0.1m$ as object radius. The object here is PEC. $\varepsilon_{sample} = -10000$ and $\mu_{sample} = 1$ **(B)** SPF of bare transformed object illuminated by far field, with radius $d' = dc/a$. In both plot working frequency is 1 GHZ.

$$\frac{k_1}{\mu_1}\left(A_{1,n} J'_n(k_1 a) + C_{1,n} H_n^{1'}(k_1 a)\right) = \frac{k_2}{\mu_2}\left(A_{2,n} J'_n(k_2 a) + C_{2,n} H_n^{1'}(k_2 a)\right) \tag{13}$$

And for continuity of magnetic fields at boundary of object inside the core medium, $\rho = d$,

$$\frac{k_2}{\mu_2}\left(A_{2,n} J'_n(k_2 d) + C_{2,n} H_n^{1'}(k_2 d)\right) = \frac{k_3}{\mu_3}\left(A_{3,n} J'_n(k_3 d)\right) \tag{14}$$

Finally, we can obtain the unknown coefficients in all regions with recursive procedure (Cheng et al., 2009) using MATLAB code. Hence, we can plot the electric field in all regions as shown in **Figure 4A**. Moreover, we can achieve $C_{0,n}$, the scattering coefficient of wave in the host medium in **Eq. 5**, in order to plot RCS in the end of this paper.

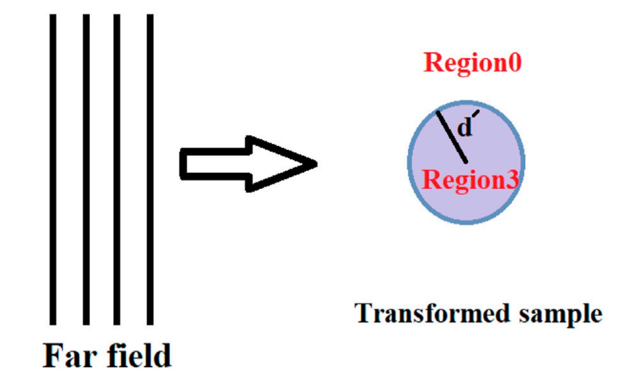

FIGURE 5 | Schematic plan for bare transformed cylinder with radius d'. $\varepsilon' = \varepsilon_{sample}c/a$ and $\mu' = \mu_{sample}c/a$ are the CP of the bare transformed object that illuminated by planewave.

Now to comprehend and understand the illusion perception, similar to the scattering calculation for the expander device, we also provide the same calculation for SFP of bare transformed cylinder as shown in **Figure 5** with transformed size and CP. For the transformed case we use a bare cylinder with radius $d' = (c/a)d$ and CP, $\varepsilon' = \varepsilon_{sample}(c/a)^2$ and $\mu' = \mu_{sample}$ illuminate by TE plane wave. We can provide the wave expansion outside of sample $\rho > d'$,

$$E_0 = \mathcal{E}\sum_{n=-\infty}^{n=\infty}\left[A_{0,n}J_n(k_0\rho) + C^t_{0,n}H^1_n(k_0 r)\right]e^{in\varphi} \tag{15}$$

Where $C^t_{0,n}$ is the scattering coefficient of wave in region0. And for inside the sample $\rho < d'$,

$$E_3 = \mathcal{E}\sum_{n=-\infty}^{n=\infty}\left[A_{3,n}J_n(k_3\rho)\right]e^{in\varphi} \tag{16}$$

In this case we have only one interface and for continuity of electric field and magnetic field we can derive matching boundary condition as follow.

For the electric fields at the boundary $r = d'$,

$$A_{0,n}J_n(k_0 d') + C_{0,n}H^1_n(k_0 d') = A_{3,n}J_n(k_3 d') \tag{17}$$

And for magnetic fields at the boundary $r = d'$,

$$\frac{k_0}{\mu_0}\left(A_{0,n}J'_n(k_0 d') + C_{0,n}H^{1'}_n(k_0 d')\right) = \frac{k_3}{\mu_3}\left(A_{3,n}J'_n(k_3 d')\right) \tag{18}$$

Similar to calculations in the expander case we calculate the unknown coefficients using recursive code and plot the electric inside and outside of the object as shown in **Figure 4B**. Illusion perception can be understood by comparing SFP in **Figure 4A** and SFP in **Figure 4B** in region $\rho > b$. In region $\rho > b$ SFP of both cases are the same as each other. Hence, we can say qualitatively, the expander creates the same illusion as a bare transformed object with transformed size and CP parameters.

Now for more consideration we also provide the same calculation for illusion perception using near field source. For this part we illuminate both the expander and bare transformed object by a point source located near the device (ρ') with working frequency 1 GHZ. Hence, we provide the total electric field in all regions.

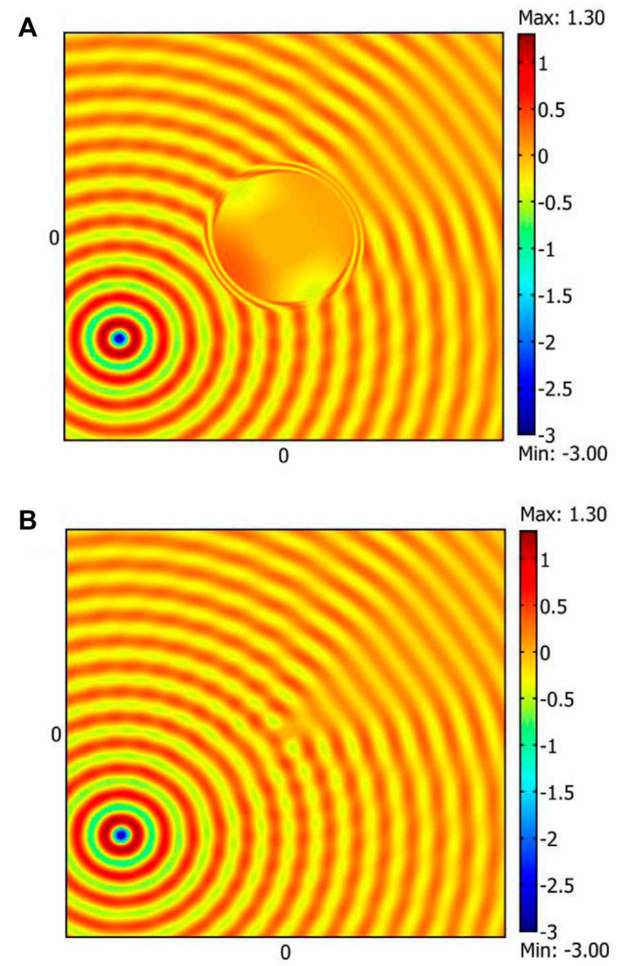

FIGURE 6 | (A) SFP of object placed in core medium of expander and illuminated by nearfield with $b = 0.3m$, $a = 0.25m$ and $c = 0.05m$ and $d = 0.1m$ as object radius. The object here is PEC. $\varepsilon_{sample} = -10000$ and $\mu_{sample} = 1$ **(B)** SPF of bare transformed object and illuminated by nearfield with radius $d' = dc/a$. In both plot working frequency is 1 GHZ and the point source located in.$\rho' = -0.6i - 0.4j$

For the expander calculation, outside of device, we can derive total electric field as follow.Where $C_{0,n}$ is the scattering parameter in region0. For electric field in surrounding shell region, $a < \rho < b$,

$$E_0(\rho,\varnothing) = \hat{a}_z\mathcal{E}\times\begin{cases}\sum_{n=-\infty}^{\infty}\left[J_n(k_0\rho)H^{(2)}_n(k_0\rho') + C_{0,n}H^{(2)}_n(k_0\rho)\right]e^{in(\varphi-\varphi')} & b\le\rho\le\rho' \\ \sum_{n=-\infty}^{\infty}\left[J_n(k_0\rho') + C_{0,n}\right]H^{(2)}_n(k_0\rho)e^{in(\varphi-\varphi')} & \rho\ge\rho'\end{cases} \tag{19}$$

$$E_1(\rho,\varphi) = \hat{a}_z\mathcal{E}\sum_{n=-\infty}^{\infty}\left\{\alpha^{C1}_n J_n(k_1\rho) + \beta^{C1}_n H^{(1)}_n(k_1\rho)e^{in(\varphi-\varphi')}\right\} \tag{20}$$

For core region, $d < \rho < a$,

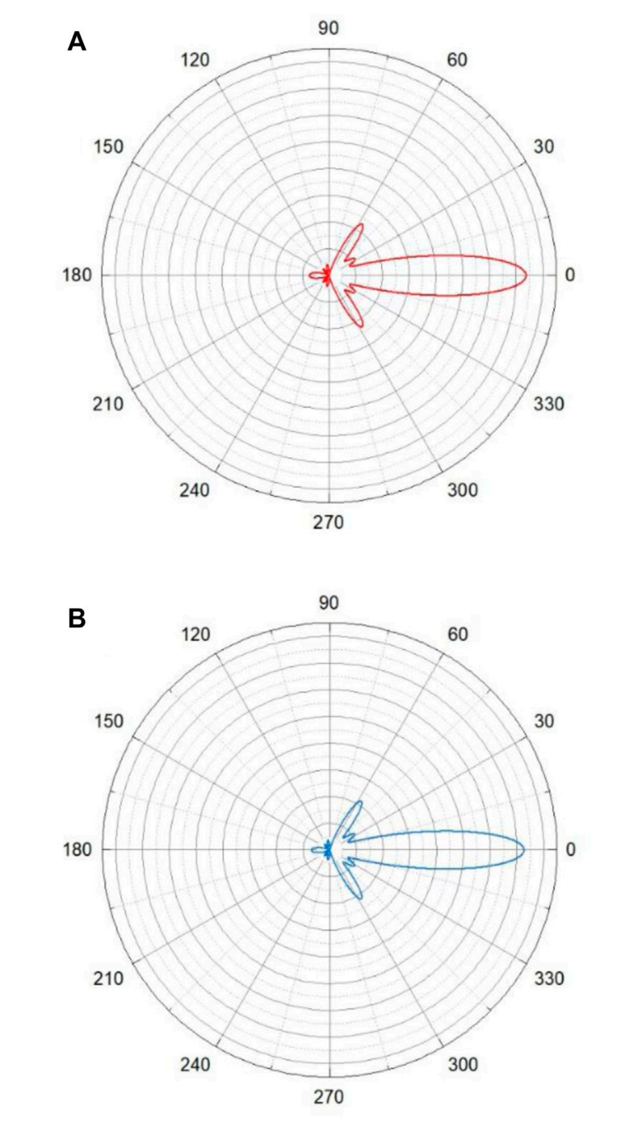

FIGURE 7 | (A) RCS (scale of 0.1 m) of a cylinder placed in expander **(B)** RCS (scale of 0.1 m) of bare transformed cylinder.

$$E_2(\rho,\varphi) = \hat{a}_z\mathcal{E}\sum_{n=-\infty}^{\infty}\left\{\alpha_n^{C2}J_n(k_2\rho) + \beta_n^{C2}H_n^{(1)}(k_2\rho)e^{in(\varphi-\varphi')}\right\} \tag{21}$$

And finally, for inside the object, $\rho < d$,

$$E_3(\rho,\varphi) = \hat{a}_z\mathcal{E}\sum_{n=-\infty}^{\infty}\left\{\alpha_n^{C3}J_n[k_3\rho]e^{in(\varphi-\varphi')}\right\} \tag{22}$$

Similar to far field calculation we use BC for continuity of electric and magnetic field at all interfaces and using recursive method (Cheng et al., 2009) we can derive all unknown parameters and plot the electric field in all regions as showed in **Figure 6A**.

Likewise, to understand and comprehend the illusion effect we have the same calculation for the bare transformed cylinder that is illuminated by point source. we can calculate the wave outside the cylinder as follow.Where $C_{0,n}^t$ is the coefficient parameter of the scattering wave and ρ' is the location of the point source. Also, for inside the cylinder we can present the following equation,

$$E_0(\rho,\varnothing) = \hat{a}_z\mathcal{E}\times\begin{cases}\sum_{n=-\infty}^{\infty}\left[J_n(k_0\rho)H_n^{(2)}(k_0\rho') + C_{0,n}^t H_n^{(2)}(k_0\rho)\right]e^{in(\varphi-\varphi')} & b\le\rho\le\rho' \\ \sum_{n=-\infty}^{\infty}\left[J_n(k_0\rho') + C_{0,n}^t\right]H_n^{(2)}(k_0\rho)e^{in(\varphi-\varphi')} & \rho\ge\rho'\end{cases} \tag{23}$$

$$E_3(\rho,\varphi) = \hat{a}_z\mathcal{E}\sum_{n=-\infty}^{\infty}\left\{\alpha_n^{C3}J_n[k_3\rho]e^{in(\varphi-\varphi')}\right\} \tag{24}$$

Similar to far field derivation we use **a** recursive method to calculate unknown parameters and plot the field inside and outside the cylinder as shown in **Figure 6B**. Also, illusion perception can be understood by comparing SFP in **Figure 6A** and **Figure 6B** i.e., the SFPs in the region $\rho \ge b$ show the same pattern in both cases qualitatively.

For more precise consideration we provide a qualitative approach. RCS is an indicator of far field scattering, SO, we use RCS plot to compare the both scattering far fields to prove the perfect illusion perception. we use scattering parameters of both object in far field to plot RCS of both scatterers using scattering formula,

$$\xi(\theta) = 4\Big/k_0\left|\sum_{n=-\infty}^{+\infty}C_n e^{in\theta}\right|^2 \tag{25}$$

We plot the RSCs in **Figures 7A, B** for expander and bare transformed cylinder, respectively. Both RSCs of samples illustrate the same scattering effects and hence, perfect illusion can be realized.

CONCLUSION

Although the wave expander transformation optic-base manipulates electromagnetic wave propagation to expand the wave in core medium, it has some illusory effects that can change the radar cross section of objects. In this paper we used scattering theory to provide full calculations and close solutions to show illusion effects of this device. For this end we compared the scattered waves from both the bare transformed object and object placed in the expander. Moreover, we provided a comparison in RCS for both objects. The results, RCSs and SFPs for both objects, confirmed the perfect illusion effects. Expander illustrates perfect illusion perception in the size of objects.

DATA AVAILABILITY STATEMENT

The raw data supporting the conclusion of this article will be made available by the authors, without undue reservation.

AUTHOR CONTRIBUTIONS

MMS conceived the idea and did the theoretical calculations and the numerical simulations. MMS wrote and revised the manuscript.

REFERENCES

Chen, H., Chan, C. T., and Sheng, P. (2010). Transformation Optics and Metamaterials. *Nat. Mater* 9, 387–396. doi:10.1038/nmat2743

Chen, H., and Chan, C. T. (2007). Transformation Media that Rotate Electromagnetic Fields. *Appl. Phys. Lett.* 90, 241105. doi:10.1063/1.2748302

Chen, H., Hou, B., Chen, S., Ao, X., Wen, W., and Chan, C. T. (2009). Design and Experimental Realization of a Broadband Transformation Media Field Rotator at Microwave Frequencies. *Phys. Rev. Lett.* 102, 183903. doi:10.1103/physrevlett.102.183903

Chen, H., Luo, X., Ma, H., and Chan, C. T. (2008). The Anti-cloak. *Opt. Express* 16, 14603–14608. doi:10.1364/oe.16.014603

Chen, H., Miao, R.-X., and Li, M. (2010). Transformation Optics that Mimics the System outside a Schwarzschild Black Hole. *Opt. Express* 18, 15183–15188. doi:10.1364/oe.18.015183

Cheng, Y., Xu, J. Y., and Liu, X.-J. (2009). Broadband Acoustic Cloak with Multilayered Homogeneous Isotropic Materials. *Piers Online* 52, 177–180.doi:10.2529/piers080901204601

Forouzeshfard, M. R., and Hosseini Farzad, M. (2018). Illusion Optics by Single and Twin Cylindrical Cavity Cloaks. *Optik* 156, 1007–1013. doi:10.1016/j.ijleo.2017.12.053

Jiang, W. X., Ma, H. F., Cheng, Q., and Cui, T. J. (2010). Illusion Media: Generating Virtual Objects Using Realizable Metamaterials. *Appl. Phys. Lett.* 96, 121910. doi:10.1063/1.3371716

Jiang, X., Liang, B., Zou, X.-Y., Yin, L.-L., and Cheng, J.-C. (2014). Broadband Field Rotator Based on Acoustic Metamaterials. *Appl. Phys. Lett.* 104, 083510. doi:10.1063/1.4866333

Jiang, Z. H., Gregory, M. D., and Werner, D. H. (2011). Experimental Demonstration of a Broadband Transformation Optics Lens for Highly Directive Multibeam Emission. *Phys. Rev. B* 84, 1–6. doi:10.1103/physrevb.84.165111

Kwon, D.-H., and Werner, D. H. (2008). Polarization Splitter and Polarization Rotator Designs Based on Transformation Optics. *Opt. Express* 16, 18731–18738. doi:10.1364/oe.16.018731

Lai, Y., Ng, J., Chen, H., Han, D., Xiao, J., Zhang, Z.-Q., et al. (2009). Illusion Optics: the Optical Transformation of an Object into Another Object. *Phys. Rev. Lett.* 102, 253902. doi:10.1103/physrevlett.102.253902

Leonhardt, U. (2006). Optical Conformal Mapping. *Science* 312, 1777–1780. doi:10.1126/science.1126493

Li, C., Liu, X., Liu, G., Li, F., and Fang, G. (2011). Experimental Demonstration of Illusion Optics with "External Cloaking" Effects. *Appl. Phys. Lett.* 99, 084104. doi:10.1063/1.3629770

Li, L., Huo, F., Zhang, Y., Chen, Y., and Liang, C. (2013). Design of Invisibility Anti-cloak for Two-Dimensional Arbitrary Geometries. *Opt. Express* 21, 9422–9427. doi:10.1364/oe.21.009422

Liu, Y., Guo, S., and He, S. (2019). Illusion Optics: Disguising with Ordinary Dielectric Materials. *Adv. Mater* 316, e1805106.

Luo, Y., Chen, H., Zhang, J., Ran, L., and Kong, J. A. (2008). Design and Analytical Full-Wave Validation of the Invisibility Cloaks, Concentrators, and Field Rotators Created with a General Class of Transformations. *Phys. Rev. B* 77, 125127. doi:10.1103/physrevb.77.125127

Mei, Z. L., Bai, J., and Cui, T. J. (2011). Experimental Verification of a Broadband Planar Focusing Antenna Based on Transformation Optics. *New J. Phys.* 13, 1367–2630. doi:10.1088/1367-2630/13/6/063028

Narimanov, E. E., and Kildishev, A. V. (2009). Optical Black Hole: Broadband Omnidirectional Light Absorber. *Appl. Phys. Lett.* 95, 041106. doi:10.1063/1.3184594

Pendry, J. B., Schurig, D., and Smith, D. R. (2006). Controlling Electromagnetic Fields. *Science* 312, 1780–1782. doi:10.1126/science.1125907

Rahm, M., Schurig, D., Roberts, D. A., Cummer, S. A., Smith, D. R., and Pendry, J. B. (2008). Design of Electromagnetic Cloaks and Concentrators Using Form-Invariant Coordinate Transformations of Maxwell's Equations. *Photonics Nanostructures - Fundam. Appl.* 6, 87–95. doi:10.1016/j.photonics.2007.07.013

Roberts, D. A., Kundtz, N., and Smith, D. R. (2009). Optical Lens Compression via Transformation Optics. *Opt. Express* 17, 16535–16542. doi:10.1364/oe.17.016535

Sadeghi, M. M. (2020). Illusion Properties in Perfect Cylindrical Devices. *Plasmonics* 153, 709–715. doi:10.1007/s11468-019-01088-4

Sadeghi, M. M., Li, S., Xu, L., Hou, B., and Chen, H. (2015). Transformation Optics with Fabry-Pérot Resonances. *Sci. Rep.* 5, 8680. doi:10.1038/srep08680

Sadeghi, M. M., Nadgaran, H., and Chen, H. (2014). Perfect Field Concentrator Using Zero Index Metamaterials and Perfect Electric Conductors. *Front. Phys.* 9, 90–93. doi:10.1007/s11467-013-0374-0

Sadeghi, M. M., Xu, L., Nadgaran, H., and Chen, H. (2015). Optical Concentrators with Simple Layered Designs. *Sci. Rep.* 5, 11015. doi:10.1038/srep11015

Schurig, D., Mock, J. J., Justice, B. J., Cummer, S. A., Pendry, J. B., Starr, A. F., et al. (2006). Metamaterial Electromagnetic Cloak at Microwave Frequencies. *Science* 314, 977–980. doi:10.1126/science.1133628

Xu, L., and Chen, H. (2015). Conformal Transformation Optics. *Nat. Phot.* 9, 15–23. doi:10.1038/nphoton.2014.307

Yan, M., Yan, W., and Qiu, M. (2008). Cylindrical Superlens by a Coordinate Transformation. *Phys. Rev. B* 78, 125113. doi:10.1103/physrevb.78.125113

Zhao, P., Cai, G., and Chen, H. (2022). Exact Transformation Optics by Using Electrostatics. *Sci. Bull.* 673, 246–255. doi:10.1016/j.scib.2021.09.017

Conflict of Interest: The authors declare that the research was conducted in the absence of any commercial or financial relationships that could be construed as a potential conflict of interest.

Publisher's Note: All claims expressed in this article are solely those of the authors and do not necessarily represent those of their affiliated organizations, or those of the publisher, the editors and the reviewers. Any product that may be evaluated in this article, or claim that may be made by its manufacturer, is not guaranteed or endorsed by the publisher.